

Article

# Constituents of *Coreopsis lanceolata* Flower and Their Dipeptidyl Peptidase IV Inhibitory Effects

Bo-Ram Kim <sup>1,2</sup>, Sunil Babu Paudel <sup>3</sup>, Joo-Won Nam <sup>3</sup> , Chang Hyun Jin <sup>1</sup> , Ik-Soo Lee <sup>2,\*</sup> and Ah-Reum Han <sup>1,\*</sup> 

<sup>1</sup> Advanced Radiation Technology Institute, Korea Atomic Energy Research Institute, Jeongseup-si, Jeollabuk-do 56212, Korea; boram1606@kaeri.re.kr (B.-R.K.); chjin@kaeri.re.kr (C.H.J.)

<sup>2</sup> College of Pharmacy, Chonnam National University, Gwangju 61186, Korea

<sup>3</sup> College of Pharmacy, Yeungnam University, Gyeongsan-si, Gyeongsangbukdo 38541, Korea; phrsunil@gmail.com (S.B.P.); jwnam@yu.ac.kr (J.-W.N.)

\* Correspondence: islee@chonnam.ac.kr (I.-S.L.); arhan@kaeri.re.kr (A.-R.H.); Tel.: +82-62-530-2932 (I.-S.L.); +82-63-570-3167 (A.-R.H.)

Academic Editor: Cristina Forzato

Received: 7 September 2020; Accepted: 22 September 2020; Published: 23 September 2020



**Abstract:** A new polyacetylene glycoside, (5*R*)-6*E*-tetradecene-8,10,12-triyn-1-ol-5-*O*- $\beta$ -glucoside (**1**), was isolated from the flower of *Coreopsis lanceolata* (Compositae), together with two known compounds, bidenoside C (**10**) and (3*S*,4*S*)-5*E*-trideca-1,5-dien-7,9,11-triyn-3,4-diol-4-*O*- $\beta$ -glucopyranoside (**11**), which were found in *Coreopsis* species for the first time. The other known compounds, lanceoletin (**2**), 3,2'-dihydroxy-4-3'-dimethoxychalcone-4'-glucoside (**3**), 4-methoxylanceoletin (**4**), lanceolin (**5**), leptosidin (**6**), (2*R*)-8-methoxybutin (**7**), luteolin (**8**) and quercetin (**9**), were isolated in this study and reported previously from this plant. The structure of **1** was elucidated by analyzing one-dimensional and two-dimensional nuclear magnetic resonance and high resolution-electrospray ionization-mass spectrometry data. All compounds were tested for their dipeptidyl peptidase IV (DPP-IV) inhibitory activity and compounds **2-4**, **6** and **7** inhibited DPP-IV activity in a concentration-dependent manner, with IC<sub>50</sub> values from 9.6 to 64.9  $\mu$ M. These results suggest that *C. lanceolata* flower and its active constituents show potential as therapeutic agents for diseases associated with type 2 diabetes mellitus.

**Keywords:** *Coreopsis lanceolata*; polyacetylene glycoside; flavonoid; dipeptidyl peptidase IV; type 2 diabetes mellitus

## 1. Introduction

*Coreopsis* is a perennial plant belonging to the Compositae family [1]. It was planted for decoration on the roadsides in North America, Asia and Oceania regions [2–4]. Typically, *C. lanceolata*, *C. tinctoria* and *C. drummondii* are generally *Coreopsis* plants distributed all around Korea [5]. Among them, *C. lanceolata* are ornamental plants commonly found in Korea in spring and summer. The shape of the yellow petals are split and jagged, and have a diameter 4–6 cm, which is larger than other species [5,6]. In the previous phytochemical studies on *C. lanceolata*, phenolics, flavonoids (aurones, chalcones, flavanols, flavanols) and acetylene compounds have been isolated from this plant [5–12]. The *C. lanceolata* flower has been reported to have diverse biological activities, such as anti-cancer [5], anti-inflammatory [6], antioxidant [6,8,10], anti-allergenic [9,10], antileukemic [11] and nematocidal [12] effects. Because of the good efficacy of *C. lanceolata*, it has been traditionally used as an ingredient in herbal medicine, such as folk remedies to control fever in China and East Asia [8]. This plant has been studied for a few chemical constituents and its pharmacological activity, but a literature review revealed that there is no anti-diabetes.

Type 2 diabetes mellitus is a chronic metabolic disorder, characterized by hyperglycemia caused by the dysregulation of blood glucose homeostasis, increased liver glucose production, insulin secretion, insulin resistance and  $\beta$ -cell dysfunction [13]. According to the eighth edition of the International Diabetes Federation (IDF) Diabetes Atlas, there were 425 million people with diabetes worldwide in 2017, and most of them have type 2 diabetes mellitus. This number of patients is increasing every year, and is expected to increase to about 700 million by 2045 [14]. The five factors that affect diabetes treatment are dipeptidyl peptidase-IV (DPP-IV),  $\alpha$ -glucosidase inhibitors, aldose reductase (ALR) inhibitors, phatase 1B (PTP1B) inhibitors and peroxisome proliferator-activated receptor- $\gamma$  (PPAR- $\gamma$ ) [15]. Recently, incretin-based therapies for the treatment of type 2 diabetes mellitus have begun to appear, one of which is DPP-IV inhibitors [16]. The incretin system includes glucagon-like peptide-1 (GLP-1) and glucose-dependent insulinotropic polypeptide (GIP), which in response to high blood sugar levels induce the release of insulin from the pancreatic  $\beta$ -cell [13,16]. DPP-IV is involved in the quick degradation and inactivation of GLP-1 and GIP in the incretin system [17]. As a result, DPP-IV inhibition enhances the glucose-producing effect of GLP-1, thereby improving glucose tolerance in diabetic patients [18]. As DPP-IV inhibitors, synthetic chemical compounds or natural product-derived compounds recently represent promising drug candidates [16,19–22].

During the screening procedure to find new candidates from natural sources for the treatment of type 2 diabetes mellitus, the ethyl acetate fraction of the *C. lanceolata* flower showed potent inhibitory activity in a DPP-IV inhibitor screening assay, with 100% inhibition at a concentration of 100  $\mu$ g/mL. Therefore, this active fraction was subjected to detailed phytochemical investigation, and 11 compounds were isolated, including a new compound **1** (Figure 1). In this study, we describe the isolation and structural elucidation of **1** and the biological results of compounds **1–11**.

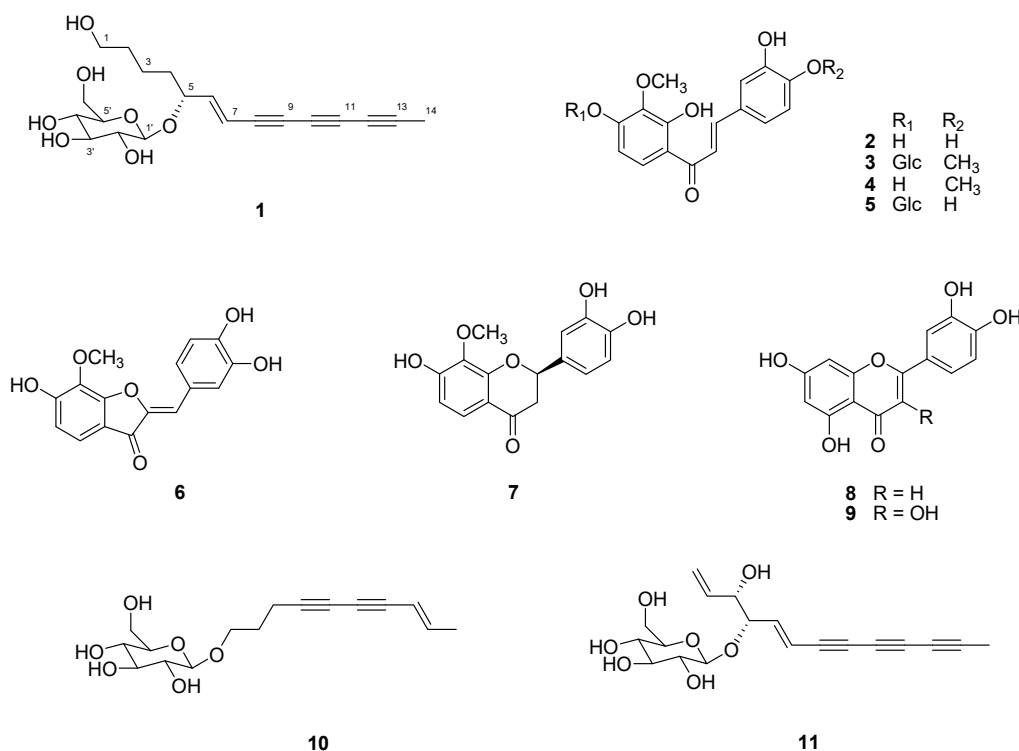


**Figure 1.** Chemical structures of compounds isolated from the ethyl acetate-soluble fraction of *Coreopsis lanceolata*.

## 2. Results and Discussion

### 2.1. Structure Elucidation of Compound 1

Compound **1** was obtained as a brown solid, with a molecular ion peak at  $m/z$  401.1575  $[M+Na]^+$  in the high resolution electrospray ionization mass spectrum, corresponding to an elemental formula of  $C_{20}H_{26}O_7Na$ . Its specific UV spectrum showed maximum absorptions at 254, 260, 274, 290, 310 and 330 nm, predicted to be ene-triayne chromophore [23,24]. The  $^1H$  NMR and  $^{13}C$  NMR spectra of **1** (Table 1) exhibited signals for a trans-olefin group at  $\delta_H$  6.39 (1H, dd,  $J = 16.0, 6.0$  Hz, H-6)/ $\delta_C$  151.4 (C-6) and  $\delta_H$  6.06 (1H, dd,  $J = 16.0, 1.5$  Hz, H-7)/ $\delta_C$  108.6 (C-7), three methylene groups at  $\delta_H$  1.45 (2H, dd,  $J = 13.0, 6.8$  Hz, H-4)/ $\delta_C$  35.1 (C-4),  $\delta_H$  1.35 (2H, dd,  $J = 14.0, 6.3$  Hz, H-2)/ $\delta_C$  32.8 (C-2), and  $\delta_H$  1.28 (2H, dd,  $J = 14.0, 6.8$  Hz, H-3)/ $\delta_C$  21.7 (C-3), an oxygenated methylene group at  $\delta_H$  3.33 (2H, dd,  $J = 12.3, 6.3$  Hz, H-1)/ $\delta_C$  61.1 (C-1), and an oxygenated methine group at  $\delta_H$  4.26 (1H, ddd,  $J = 13.0, 6.0, 1.5$  Hz, H-5)/ $\delta_C$  76.5 (C-5), representing a 6-heptene-1,5-diol group, which was supported by the  $^1H$ - $^1H$  COSY correlations of H-1/H-2, H-4/H-3, H-5 and H-6/H-5, H-7, and the  $^1H$ - $^{13}C$  HMBC correlations of H-1/C-3, H-2/C-4 and H-4/C-6 (Figure 2). Additional signals for a methyl group at  $\delta_H$  2.02 (3H, s, H-14)/ $\delta_C$  4.6 (C-14) and six acetylene carbons at  $\delta_C$  81.3 (C-13), 75.4 (C-8), 74.0 (C-9), 64.6 (C-12), 67.4 (C-11) and 59.0 (C-10) indicated the presence of a 1,3,5-heptatriyne group, which was attached at the trans-olefin group by the  $^1H$ - $^{13}C$  HMBC NMR correlations of H-7/C-9 and H-14/C-12. The  $^1H$  NMR and  $^{13}C$  NMR spectra of **1** also displayed signals for sugar moiety at  $\delta_C$  77.4 (C-5'), 77.3 (C-3'), 74.0 (C-2'), 70.6 (C-4') and 61.7 (C-6'), including the anomeric signal at  $\delta_H$  4.00 (1H, d,  $J = 8.0$  Hz, H-1')/ $\delta_C$  101.3 (C-1'), and the sugar moiety was determined as  $\beta$ -glucopyranoside by the  $^1H$ - $^1H$  NOESY correlations of H-1'/H-3' and H-5', and H-2'/H-4' [25,26]. In the  $^1H$ - $^{13}C$  HMBC NMR spectrum, the hemiacetal proton H-1' showed a key correlation with C-5, suggesting that the  $\beta$ -glucopyranoside was positioned at C-5 in the polyacetylene aglycone. An absolute configuration of **1** at C-5 was assigned by comparing its experimental circular dichroism (CD) data with the literature data [27]. In the literature, polyacetylene glycosides established their absolute configurations by comparison of the calculated and experimental ECD spectra. According to the Sznatzke's helicity rule, the negative Cotton effect at 300–320 nm permitted the configuration of the glucoside-attached carbon to *R*, while the positive Cotton effect at 300–320 nm permitted the configuration of the glucoside-attached carbon to *S*. Based on this observation (Figures S8 and S9), the absolute configuration of **1** was determined as (5*R*). Therefore, the structure of **1** was elucidated as (5*R*)-6*E*-tetradecene-8,10,12-triayne-1-ol-5-*O*- $\beta$ -glucoside (**1**), which is a new polyacetylene glycoside.

**Table 1.**  $^1H$ -NMR (500 MHz) and  $^{13}C$ -NMR (125 MHz) spectral data (DMSO- $d_6$ ,  $\delta$  in ppm) of **1** isolated from *Coreopsis lanceolata*.

Position	1		
	$\delta_H$	$\delta_C$	HMBC (Carbon No.)
1	3.33 (2H, dd, $J = 12.3, 6.3$ )	61.1	3
2	1.35 (2H, dd, $J = 14.0, 6.3$ )	32.8	4
3	1.28 (2H, dd, $J = 14.0, 6.8$ )	21.7	5
4	1.45 (2H, dd, $J = 13.0, 6.8$ )	35.1	6
5	4.26 (1H, ddd, $J = 13.0, 6.0, 1.5$ )	76.5	1', 7
6	6.39 (1H, dd, $J = 16.0, 6.0$ )	151.4	8
7	6.06 (1H, dd, $J = 16.0, 1.5$ )	108.6	9, 10
8		75.5	
9		74.0	
10		59.0	
11		67.4	
12		64.6	
13		81.3	
14	2.02 (3H, s)	4.6	10, 11, 12
1'	4.00 (1H, d, $J = 8.0$ )	101.3	5, 6
2'	2.92 (1H, dd, $J = 8.0, 4.5$ )	74.0	
3'	3.07 (1H, dd, $J = 8.7, 4.5$ )	77.3	
4'	2.99 (1H, m)	70.6	
5'	2.99 (1H, m)	77.4	
6'	3.38 (1H, m)	61.7	
	3.61 (1H, dd, $J = 11.4, 6.0$ Hz)		

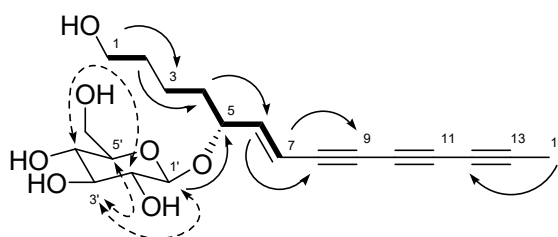


**Figure 2.** Key  $^1\text{H}$ - $^1\text{H}$  COSY (---),  $^1\text{H}$ - $^1\text{H}$  NOESY (—), and  $^1\text{H}$ - $^{13}\text{C}$  HMBC (→) correlations of **1**.

The 10 known compounds were identified as lanceoletin (**2**) [11], 3,2'-dihydroxy-4-3'-dimethoxychalcone-4'-glucoside (**3**) [8], 4-methoxylanceoletin (**4**) [11], lanceolin (**5**) [10], leptosidin (**6**) [11], (2*R*)-8-methoxybutin (**7**) [11], luteolin (**8**) [28], quercetin (**9**) [29], bidenoside C (**10**) [30] and (3*S*,4*S*)-5*E*-trideca-1,5-dien-7,9,11-triyn-3,4-diol-4-*O*- $\beta$ -glucopyranoside (**11**) [31] by comparing their spectroscopic data with published data. Flavanone **7** showed the negative Cotton effect at 295–310 nm and the positive Cotton effect at 280–290 nm in its CD spectrum, indicating a 2*R* configuration [32] (Figure S10). The absolute configuration of **11** at C-3 and C-4 was assigned by comparing its experimental CD data with the data in the literature [27], as described above for the absolute configuration determination of **1**. Compound **11** was a diastereomer and the threo stereochemistry between H-3 and H-4 was deduced by their large coupling constant ( $J = 5.5$  Hz, in methanol- $d_4$ ). The positive Cotton effect at 300–320 nm in the CD spectrum of **11** was attributed to a (3*S*,4*S*) configuration for **11** (Figure S11). Although the known compounds (**2**–**9**) have been isolated from the *Coreopsis* species, the isolation of compounds **10** and **11** from the *Coreopsis* species has not been reported yet.

## 2.2. Biological Activity

The methanol extract and solvent fractions of *C. lanceolata* confirmed their anti-diabetic effect using an in vitro DPP-IV inhibitor screening assay. The methanol extract inhibited DPP-IV activity with 87.2% inhibition at 100  $\mu\text{g}/\text{mL}$ . Thus, it was partitioned with hexanes, ethyl acetate and *n*-butanol, successively, and these solvent fractions were screened for their DPP-IV inhibition at 100  $\mu\text{g}/\text{mL}$  concentrations. Since the ethyl acetate fraction inhibited DPP-IV activity with 100% inhibition, we conducted a detailed phytochemical investigation, leading to the isolation of 11 compounds. All isolates were evaluated for their DPP-IV inhibitory effects, and compounds **2**–**4**, **6** and **7** inhibited DPP-IV activity in a concentration-dependent manner, with  $\text{IC}_{50}$  values of 9.6, 14.3, 21.6, 13.3 and 64.9  $\mu\text{M}$ , respectively (Figure 3). The positive control, sitagliptin, exhibited an  $\text{IC}_{50}$  of 0.071  $\mu\text{M}$ .

Compounds **2**–**5** have the chalcone skeleton, which is an  $\alpha$ - $\beta$ -unsaturated ketone with two phenyl rings. There have been several reviews on the biological and pharmacological activities of chalcones, including anti-cancer, anti-malarial, anti-microbial, anti-inflammatory, anti-protozoal and anti-HIV activities [33], as well as its role in diabetes control [15,34,35]. In a comprehensive study into modulating the therapeutic targets PPAR- $\gamma$ , DPP-IV,  $\alpha$ -glucosidase, PTP1B, ALR and insulin secretion via anti-diabetic chalcones and their structure–activity relationships [15], in particular, it was reported that the chalcone structure of which the carbonyl group was replaced with an oxime function exhibited enhanced DPP-IV inhibitory activity. In addition, there have been reports that nitrochalcones and prenylated chalcones increase insulin secretion and glucose uptake, respectively [34]. Among chalcones isolated in this study, **3**–**5** showed less inhibitory activity than **2**, indicating that chalcones substituted with additional methoxy group and/or sugar are less effective. The most active compound, **2**, has been reported as having various biological activities such as antileukemic [11], antioxidant [4] and anti-cancer [5], however its DPP-IV potential has not been studied previously. Compounds **6** and **7**, with the structures of aurone and flavanone, respectively, exhibited moderate DPP-IV inhibitory effects, while flavone (**8**), flavonol (**9**) and polyacetylenes (**1**, **10** and **11**) did not show their activities. The evaluation of the inhibitory activities of **1**–**11** against DPP-IV was reported for the first time in this study.

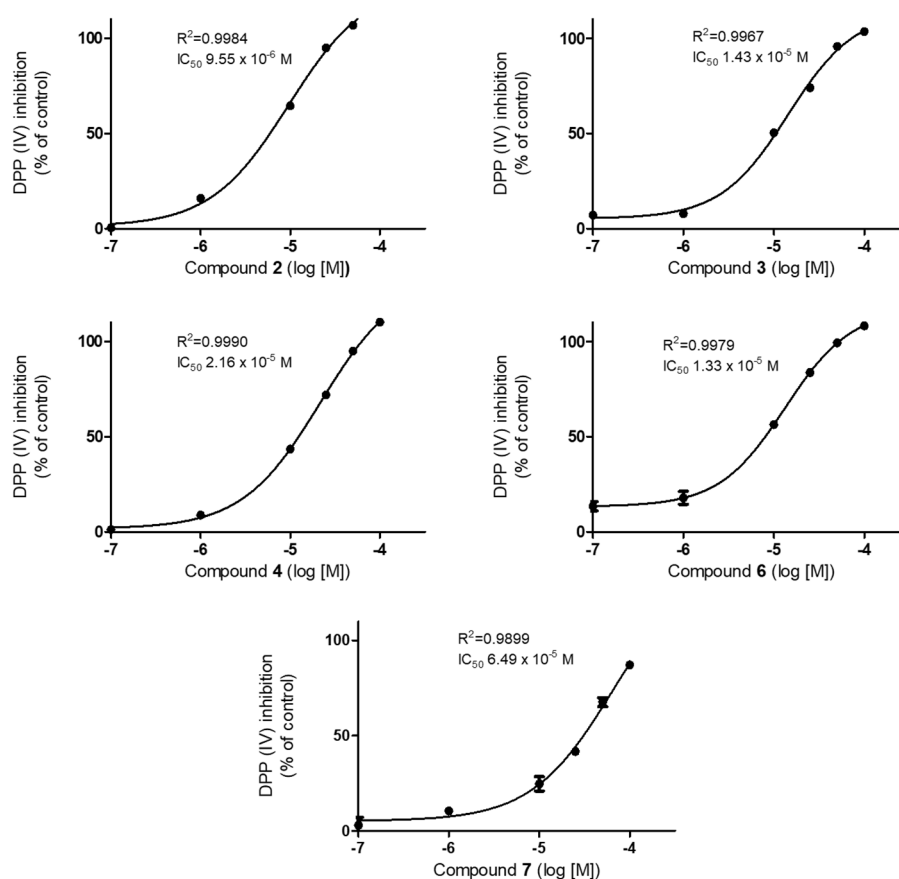


**Figure 3.** Effects of compounds 2–4, 6 and 7 on DPP-IV activity. Values are presented as the mean  $\pm$  SD of three independent experiments.

Extensive studies on the phytochemical-based DPP-IV inhibitors were undertaken in the literature [19–21], and in our previous studies [16,22]. Flavonoids and phenolic compounds were found to be the DPP-IV inhibitors with potent to mild activities, showing  $IC_{50}$  values in the range of 0.12 to 63.26  $\mu$ M. Although naturally occurring compounds were relatively less active than the synthetic DPP-IV inhibitors diprotin A and sitagliptin, the natural products with structural diversity could be useful for discovering safer DPP-IV inhibitors. Therefore, these results suggest that compounds 2–4, 6 and 7 have the potential for the development of naturally derived DPP-IV inhibitors for the treatment of type 2 diabetes mellitus and hyperglycemia, although a further study of their mechanisms of action is necessary, using in vitro and in vivo models.

### 3. Materials and Methods

#### 3.1. General Procedures

The optical rotations were measured by a JASCO DIP-1000 polarimeter (JASCO Co., Tokyo, Japan). The circular dichroism (CD) measurements were conducted using a JASCO J-810 CD-ORD spectropolarimeter (JASCO Co., Tokyo, Japan). The 1D and 2D NMR spectra were obtained from a JNM-ECA 500 MHz NMR instrument (JEOL Ltd., Tokyo, Japan). Tetramethylsilane (TMS) was used as an internal standard. High-resolution electrospray ionization mass spectra (HRESIMS) were obtained from a Waters SYNAPT G2 mass spectrometer (Waters, Milford, CT, USA). Column chromatography (CC) was performed on columns containing silica gel (70–230 mesh, Merck, Darmstadt, Germany), RP-18 (YMC gel ODS-A, 12 nm, S-75  $\mu$ m, YMC Co., Tokyo, Japan) and Sephadex LH-20 (GE Healthcare Bio-Sciences, Uppsala, Sweden). Thin-layer chromatographic (TLC) analysis was performed on Kieselgel 60 F<sub>254</sub> (Merck, Darmstadt, Germany) and Kieselgel 60 RP-18-F<sub>254S</sub> (Merck, Darmstadt,

Germany). Analytical plates were visualized under UV light (254 and 365 nm) and sprayed with 10% (*v/v*) sulfuric acid in water, followed by heating at 180 °C for 2 min. A YMC-Pack Pro C<sub>18</sub> column (5 μm, 250 mm × 20 mm i.d., YMC Co. Tokyo, Japan) was utilized for preparative high performance liquid chromatography (HPLC), operated on a Gilson Preparative HPLC system (Gilson Inc., Middleton, WI, USA). Medium pressure liquid chromatography (MPLC) was performed on a CombiFlash Rf200 system (Teledyne ISCO, Lincoln, NE, USA) with RediSep Rf Normal Phase Silica columns.

### 3.2. Plant Material

*Coreopsis lanceolata* flowers were collected at the road side around Korea Atomic Energy Research Institute, Jeonguep-si, Jeollabuk-do 56212, Korea, in June 2017. These flowers were handpicked and randomly collected at the stage of fully open flowering, then were freeze-dried and stored at −20 °C in polyethylene plastic bags until further analysis. This plant was identified by Ah-Reum Han, one of the co-authors of this study. The voucher specimens (No. Con013) were deposited at the Radiation Breeding Research Center, Advanced Radiation Technology Institute, Korea Atomic Energy Research Institute.

### 3.3. Extraction and Isolation

Freeze-dried flowers (500 g) of *C. lanceolata* were extracted with MeOH (3 × 5 L) overnight at room temperature. The solvent was evaporated in vacuo to afford an MeOH extract (201.5 g) which was then suspended in distilled water (1 L) and partitioned with hexanes (3 × 1 L), ethyl acetate (3 × 1 L) and *n*-butanol (3 × 1 L) sequentially. The EtOAc-soluble fraction (25.2 g) was then subjected to reverse-phase-C18 column chromatography (RP-C18 CC) using a gradient solvent system of MeOH-H<sub>2</sub>O (1:1 to 1:0, *v/v*) to afford 9 fractions (F01–F09). Fraction F03 (1.7 g) was subjected to RP-C18 CC with a solvent system of MeOH-H<sub>2</sub>O (1:1 to 1:0, *v/v*), affording 13 subfractions (F0301–F0313). Subfraction F0306 (546 mg) was subjected to silica gel CC with a solvent system of CH<sub>2</sub>Cl<sub>2</sub>-MeOH (9:1 to 0:1, *v/v*) to produce 14 subfractions (F030601–F030614) together with purified compound 7 (2.7 mg). Subfraction F030614 was chromatographed on RP-C18 CC with a gradient solvent system of CH<sub>3</sub>CN-H<sub>2</sub>O (4:6 to 1:0, *v/v*) to obtain 3 (20 mg). Subfraction F0311 (44 mg) was purified by RP-C18 CC with a gradient solvent system of CH<sub>3</sub>CN-H<sub>2</sub>O (4:6 to 1:0, *v/v*) to yield 6 (1.0 mg). Fraction F07 (623 mg) was subjected to RP-C18 CC with a solvent system of CH<sub>3</sub>CN-H<sub>2</sub>O (4:6 to 1:0, *v/v*), affording 18 subfractions (F0701–F0718). Subfraction F0711 (20 mg) was chromatographed on a Sephadex LH-20 column using 100% MeOH to give 8 (3.0 mg) and 9 (2.5 mg). Subfraction F0705 (77 mg) was subjected to a Sephadex LH-20 column using 100% MeOH, affording six subfractions (F0701–F0706). Subfraction F070505 (25 mg) was chromatographed on silica gel CC with a solvent system of CH<sub>2</sub>Cl<sub>2</sub>-MeOH-H<sub>2</sub>O (9:1:0.1 to 0:1:0, *v/v*) to obtain 5 (2.5 mg). Subfraction F0708 (55 mg) was subjected to a Sephadex LH-20 column using 100% MeOH, affording six subfractions (F0701–F0706). Subfraction F0708 (55 mg) was subjected to a Sephadex LH-20 column using 100% MeOH to obtain 10 (2.0 mg). F09 (900 mg) was separated by MPLC (CHCl<sub>3</sub>-MeOH, 9:1 to 0:1, 15 mL/min), affording 16 subfractions (F0901–F0916). Subfraction F0901 was purified by Sephadex LH-20 CC using 100% MeOH to yield 4 (6.0 mg). Subfraction F0904 (21 mg) was chromatographed on a Sephadex LH-20 column using 100% MeOH to give 2 (2.7 mg). Subfraction F0910 (22 mg) was purified by a Sephadex LH-20 column using 100% MeOH to give 11 (4.0 mg). Subfraction F0912 (28 mg) was chromatographed on a Sephadex LH-20 column using 100% MeOH to give 1 (2.0 mg).

(5*R*)-6*E*-tetradecene-8,10,12-triyn-1-ol-5-*O*-β-glucoside (**1**): Brown solid.  $[\alpha]_D^{26} -11.5^\circ$  (*c* 0.13, MeOH). CD (MeOH)  $\lambda_{\max}$  ( $\Delta\epsilon$ ) 228 (+0.52), 243 (−0.83), 286 (−0.11), 307 (−0.26) nm. <sup>1</sup>H (500 MHz) and <sup>13</sup>C (125 MHz) data (CD<sub>3</sub>OD), see Table 1 and Figures S1–S6. HRESIMS (positive ions) *m/z* 401.1575 [M+Na]<sup>+</sup> (calculated for C<sub>20</sub>H<sub>26</sub>O<sub>7</sub>Na, 401.1575) (Figure S7).

(2*R*)-methoxybutin (**7**): Yellow powder.  $[\alpha]_D^{26} -117.9^\circ$  (*c* 0.09, MeOH). CD (MeOH)  $\lambda_{\max}$  ( $\Delta\epsilon$ ) 275 (−0.11), 289 (+0.19), 300 (−0.23) nm.

(3*S*,4*S*)-5*E*-trideca-1,5-dien-7,9,11-triyn-3,4-diol-4-*O*- $\beta$ -glucopyranoside (**11**): Brown solid.  $[\alpha]_D^{26} +82.1^\circ$  (*c* 0.09, MeOH). CD (MeOH)  $\lambda_{\max}$  ( $\Delta\epsilon$ ) 226 (−2.50), 253 (+1.33), 290 (+0.67), 309 (+0.78) nm.

### 3.4. DPP-IV Inhibitory Activity Assay

The measurement of DPP-IV activity was performed using the DPP-IV inhibitor screening assay kit (Cayman Chemical, Ann Arbor, Michigan, USA), based on the manufacturer's protocols (Cayman Chemical). Briefly, a DPP assay buffer consisting of 20 mM Tris-HCL (pH 8.0), 100 nM NaCl and 1 mM EDTA was used for the assay solution. Each of the compounds were initially dissolved in DMSO at a concentration of 1 mM. Subsequently, the final concentration of compounds was diluted to 0.1, 1, 10, 25, 50 and 100  $\mu$ M, respectively. The human recombinant DPP-IV enzyme and the substrate 5 mM H-Gly-Pro conjugated to aminomethylcoumarin (AMC) were put in the same buffer. Diluted assay buffer (30  $\mu$ L) and diluted enzyme solution (10  $\mu$ L) were added to a 96-well plate containing 10  $\mu$ L of solvent (blank) or 10  $\mu$ L of solvent-dissolved test compounds. The reaction by adding 50  $\mu$ L of the diluted solution of the fluorogenic substrate was initiated and cleavage of the peptide bond by DPP released the free AMC group. The fluorescence was measured as an excitation wavelength of 350 nm and an emission wavelength of 450 nm using a plate reader (TECAN, Männedorf, Switzerland). The percentage inhibition was expressed as [(DPP-IV level of vehicle-treated control − DPP-IV level of test samples)/DPP-IV level of vehicle-treated control]  $\times$  100. Subsequently, the 50% inhibitory concentration (IC<sub>50</sub>) was determined using GraphPad Prism software (GraphPad Software, La Jolla, CA, USA) via a dose–response analysis.

## 4. Conclusions

A new polyacetylene glycoside, namely (5*R*)-6*E*-tetradecene-8,10,12-triyn-1-ol-5-*O*- $\beta$ -glucoside (**1**), was isolated from the *C. lanceolata* flower, along with 10 known compounds. Other polyacetylene glycosides, bidenoside C (**10**) and (3*S*,4*S*)-5*E*-trideca-1,5-dien-7,9,11-triyn-3,4-diol-4-*O*- $\beta$ -glucopyranoside (**11**), were found in the *Coreopsis* species for the first time. In the screening for any DPP-IV inhibitory activity of the isolates **1–11**, compounds **2–4**, **6** and **7** inhibited DPP-IV enzyme activity in a dose-dependent manner. This study provides the first demonstration of the compounds responsible for the DPP-IV inhibitory activity of the *C. lanceolata* flower. Moreover, lanceoletin (**2**) exhibited the most DPP-IV inhibitory effect; thus our results suggest that **2** could be considered as a lead compound for the development of agents against DPP-IV activity.

**Supplementary Materials:** The following are available online, Figure S1: <sup>1</sup>H NMR (500 MHz) spectrum of compound **1** in DMSO-*d*<sub>4</sub>, Figure S2: <sup>13</sup>C NMR (125 MHz) spectrum of compound **1** in DMSO-*d*<sub>4</sub>, Figure S3: <sup>1</sup>H-<sup>1</sup>H COSY NMR (500 MHz) spectrum of compound **1** in DMSO-*d*<sub>4</sub>, Figure S4: <sup>1</sup>H-<sup>1</sup>H NOESY NMR (500 MHz) spectrum of compound **1** in DMSO-*d*<sub>4</sub>, Figure S5: <sup>1</sup>H-<sup>1</sup>H HSQC NMR (500 MHz) spectrum of compound **1** in DMSO-*d*<sub>4</sub>, Figure S6: <sup>1</sup>H-<sup>1</sup>H HMBC NMR (500 MHz) spectrum of compound **1** in DMSO-*d*<sub>4</sub>, Figure S7: The HR-ESI-MS data of **1**, Figure S8: The UV spectrum of **1** in methanol, Figure S9: The CD spectrum of **1** in methanol, Figure S10: The CD spectrum of **7** in methanol, Figure S11: The CD spectrum of **11** in methanol.

**Author Contributions:** Conceptualization, B.-R.K. and A.-R.H.; methodology, B.-R.K., C.H.J., S.B.P., J.-W.N. and A.-R.H.; software, B.-R.K. and S.B.P.; validation, C.H.J., J.-W.N. and A.-R.H.; formal analysis, B.-R.K. and S.B.P.; investigation, B.-R.K. and S.B.P.; resources, B.-R.K. and A.-R.H.; data curation, B.-R.K. and S.B.P.; writing—original draft preparation, B.-R.K. and A.-R.H.; writing—review and editing, B.-R.K., J.-W.N. and A.-R.H.; visualization, B.-R.K. and S.B.P.; supervision, I.-S.L. and A.-R.H.; project administration, C.H.J.; funding acquisition, C.H.J. All authors have read and agreed to the published version of the manuscript.

**Funding:** This research was supported by Radiation Technology R&D program (No. 2017M2A2A6A05018541) through the National Research Foundation of Korea (NRF) funded by the Ministry of Science, ICT & Future Planning.

**Acknowledgments:** The authors thank the Core Research Support Center for Natural Products and Medical Materials (CRCNM) for technical support for optical rotation and CD experiments.

**Conflicts of Interest:** The authors declare no conflict of interest.

## References

1. Panero, J.L.; Funk, V.A. Toward a phylogenetic subfamilial classification for the Compositae (Asteraceae). *Proc. Biol. Soc. Wash* **2002**, *115*, 760–773.
2. Kim, S.-C.; Crawford, D.J.; Tadesse, M.; Berbee, M.; Ganders, F.R.; Pirseyedi, M.; Esselman, E.J. ITS sequences and phylogenetic relationships in *Bidens* and *Coreopsis* (Asteraceae). *Syst. Bot.* **1999**, *24*, 480–493. [[CrossRef](#)]
3. Yang, Y.; Sun, X.; Liu, J.; Kang, L.; Chen, S.; Ma, B.; Guo, B. Quantitative and qualitative analysis of flavonoids and phenolic acids in snow chrysanthemum (*Coreopsis tinctoria* Nutt.) by HPLC-DAD and UPLC-ESI-QTOF-MS. *Molecules* **2016**, *21*, 1307. [[CrossRef](#)] [[PubMed](#)]
4. Nakabo, D.; Okano, Y.; Kandori, N.; Satahira, T.; Kataoka, N.; Akamatsu, J.; Okada, Y. Convenient synthesis and physiological activities of flavonoids in *Coreopsis lanceolata* L. Petals and their related compounds. *Molecules* **2018**, *23*, 1671. [[CrossRef](#)] [[PubMed](#)]
5. Kim, H.-G.; Oh, H.-J.; Ko, J.-H.; Song, H.S.; Lee, Y.-G.; Kang, S.C.; Lee, D.Y.; Baek, N.-I. Lanceolein A-G, hydroxychalcones, from the flowers of *Coreopsis lanceolata* and their chemopreventive effects against human colon cancer cells. *Bioorg. Chem.* **2019**, *85*, 274–281. [[CrossRef](#)] [[PubMed](#)]
6. Kim, H.-G.; Jung, Y.S.; Oh, S.M.; Oh, H.-J.; Ko, J.-H.; Kim, D.-O.; Kang, S.C.; Lee, Y.-G.; Baek, N.-I. Coreolanceolins A-E, new flavanones from the flowers of *Coreopsis lanceolata*, and their antioxidant and anti-inflammatory effects. *Antioxidants* **2020**, *9*, 539. [[CrossRef](#)] [[PubMed](#)]
7. Okada, Y.; Okita, M.; Murai, Y.; Okano, Y.; Nomura, M. Isolation and identification of flavonoids from *Coreopsis lanceolata* L. pentals. *Nat. Prod. Res.* **2014**, *28*, 201–204. [[CrossRef](#)]
8. Shang, Y.F.; Oidovsambuu, S.; Jeon, J.-S.; Nho, C.W.; Um, B.-H. Chalcones from flowers of *Coreopsis lanceolata* and their in vitro antioxidative activity. *Planta Med.* **2013**, *79*, 295–300.
9. Shao, D.; Zheng, D.; Hu, T.; Chen, W.; Chen, D.; Zhuo, X. Chemical constituents from *Coreopsis lanceolata*. *Zhongcaoyao* **2013**, *44*, 1558–1561.
10. Tanimoto, S.; Miyazawa, M.; Inoue, T.; Okada, Y.; Nomura, M. Chemical constituents of *Coreopsis lanceolata* L. and their physiological activities. *J. Oleo Sci.* **2009**, *58*, 141–146. [[CrossRef](#)]
11. Pardede, A.; Mashita, K.; Ninomiya, M.; Tanaka, K.; Koketsu, M. Flavonoid profile and antileukemic activity of *Coreopsis lanceolata* flowers. *Bioorg. Med. Chem. Lett.* **2016**, *26*, 2784–2787. [[CrossRef](#)] [[PubMed](#)]
12. Kimura, Y.; Hiraoka, K.; Kawano, T.; Fujioka, S.; Shimada, A. Nematicidal activities of acetylene compounds from *Coreopsis lanceolata* L. *J. Biosci.* **2008**, *63*, 843–847. [[CrossRef](#)] [[PubMed](#)]
13. Nauck, M. Incretin therapies: Highlighting common features and differences in the modes of action of glucagon-like peptide-1 receptor agonists and dipeptidyl peptidase-4 inhibitors. *Diabetes Obes. Metab.* **2016**, *18*, 203–216. [[CrossRef](#)] [[PubMed](#)]
14. Ma, Q.; Li, Y.; Wang, M.; Tang, Z.; Wang, T.; Liu, C.; Wang, C.; Zhao, B. Progress in metabolomics of type 2 diabetes mellitus. *Molecules* **2018**, *23*, 1834. [[CrossRef](#)]
15. Mahapatra, D.K.; Asati, V.; Bharti, S.K. Chalcones and their therapeutic targets for the management of diabetes: Structural and pharmacological perspectives. *Eur. J. Med. Chem.* **2015**, *92*, 839–865. [[CrossRef](#)]
16. Kim, B.-R.; Kim, H.Y.; Choi, I.H.; Kim, J.-B.; Jin, C.H.; Han, A.-R. DPP-IV inhibitory potentials of flavonol glycosides isolated from the seeds of *Lens culinaris*: In vitro and molecular docking analyses. *Molecules* **2018**, *23*, 1998. [[CrossRef](#)]
17. Mentlein, R. Dipeptidyl-peptidase IV (CD-26) role in the inactivation of regulatory peptides. *Regul. Pept.* **1999**, *85*, 9–24. [[CrossRef](#)]
18. Langley, A.K.; Suffoletta, T.J.; Jennings, H.R. Dipeptidyl-peptidase IV inhibitors and the incretin system in type 2 diabetes mellitus. *Pharmacotherapy* **2007**, *27*, 1163–1180. [[CrossRef](#)]
19. Kerru, N.; Singh-Pillay, A.; Awolade, P.; Singh, P. Current anti-diabetic agents and their molecular targets: A review. *Eur. J. Med. Chem.* **2018**, *152*, 436–488. [[CrossRef](#)]
20. Fan, J.F.; Johnson, M.H.; Lila, M.A.; Yousef, G.; de Mejia, E.G. Berry and citrus phenolic compounds inhibit dipeptidyl peptidase IV: Implications in diabetes management. *Evid. Based Complement. Alternat. Med.* **2013**, *2013*, 1–13. [[CrossRef](#)]
21. Bower, A.M.; Real Hernandez, L.M.; Berhow, M.A.; de Mejia, E.G. Bioactive compounds from culinary herbs inhibit a molecular target for type-2 diabetes management, dipeptidyl peptidase-IV. *J. Agric. Food Chem.* **2014**, *62*, 6147–6158. [[PubMed](#)]

22. Kim, B.-R.; Thapa, P.; Kim, H.M.; Jin, C.H.; Kim, S.H.; Kim, J.-B.; Choi, H.J.; Han, A.-R.; Nam, J.-W. Purification of phenylpropanoids from the scaly bulbs of *lilium longiflorum* by CPC and determination of their DPP- IV inhibitory potentials. *ACS Omega* **2020**, *5*, 4050–4057. [[PubMed](#)]
23. Silva, D.B.; Rodrigues, E.D.; Silva, G.V.J.; Lopes, N.P.; Oliveira, D.C.R. Post-column sodiation to enhance the detection of polyacetylene glycosides in LC-DAD-MS analyses: An example from *Bidens gardneri* (Asteraceae). *Talanta* **2015**, *135*, 87–93. [[PubMed](#)]
24. Guo, J.; Wang, A.; Yang, K.; Ding, H.; Hu, Y.; Yang, Y.; Huang, S.; Xu, J.; Liu, T.; Yang, H.; et al. Isolation, characterization and antimicrobial activities of polyacetylene glycosides from *Coreopsis tinctoria* Nutt. *Phytochemistry* **2017**, *136*, 1–5.
25. Saito, Y.; Takiguchi, K.; Gong, X.; Kuroda, C.; Tori, M. Thiophene, furans and related aromatic compounds from *Eupatorium heterophyllum*. *Nat. Prod. Commun.* **2011**, *6*, 361–366. [[PubMed](#)]
26. Snatos, S.C.; Carvalho, A.G.; Fortes, G.A.C.; Ferri, P.H.; de Oliveira, A.E. Variable-temperature NMR and conformational analysis of oenothein B. *J. Braz. Chem. Soc.* **2014**, *25*, 282–289.
27. Xu, K.; Yang, P.-F.; Yang, Y.-N.; Feng, Z.-M.; Jiang, J.-S.; Zhang, P.-C. Direct assignment of the *threo* and *erythro* configurations in polyacetylene glycosides by <sup>1</sup>H NMR spectroscopy. *Org. Lett.* **2017**, *19*, 686–689.
28. Lavault, M.; Richomme, P. Constituents of *Helichrysum stoechas* variety *olonnes*. *Chem. Nat. Compd.* **2004**, *10*, 118–121.
29. Kyriakou, E.; Primikyri, A.; Charisiadis, P.; Katsoura, M.; Gerothanassis, I.P.; Stamatis, H.; Txakos, A.G. Unexpected enzyme-catalyzed regioselective acylation of flavonoid aglycones and rapid product screening. *Org. Biomol. Chem.* **2012**, *10*, 1739–1742.
30. He, J.; Shen, Y.; Jiang, J.-S.; Yang, Y.-N.; Feng, Z.-M.; Zhang, P.-C.; Yuan, S.-P.; Hou, Q. New polyacetylene glucosides from the florets of *Carthamus tinctorius* and their weak anti-inflammatory activities. *Carbohydr. Res.* **2011**, *345*, 1903–1908.
31. Xi, F.-M.; Li, C.-T.; Han, J.; Yu, S.-S.; Wu, Z.-J.; Chen, W.-S. Thiophenes, polyacetylenes and terpenes from the aerial parts of *Eclipta prostrata*. *Bioorg. Med. Chem.* **2014**, *22*, 6515–6522. [[CrossRef](#)] [[PubMed](#)]
32. Slade, D.; Ferreira, D.; Marais, J.P.J. Circular dichroism, a powerful tool for the assessment of absolute configuration of flavonoids. *Phytochemistry* **2005**, *66*, 2177–2215. [[CrossRef](#)] [[PubMed](#)]
33. Singh, P.; Anand, A.; Kumar, V. Recent developments in biological activities of chalcones: A mini review. *Eur. J. Med. Chem.* **2014**, *85*, 758–777. [[CrossRef](#)] [[PubMed](#)]
34. Soares, J.M.D.; Pereira Leal, A.E.B.; Silva, J.C.; Almeida, J.R.G.S.; de Oliveira, H.P. Influence of flavonoids on mechanism of modulation of insulin secretion. *Pharmacogn. Mag.* **2017**, *13*, 639–646. [[PubMed](#)]
35. Bak, E.J.; Park, H.G.; Lee, C.H.; Lee, T.-I.; Woo, G.-H.; Na, Y.H.; Yoo, Y.-J.; Cha, J.-H. Effect of novel chalcone derivative  $\alpha$ -glucosidase, dipeptidyl peptidase-4, and adipocyte differentiation in vitro. *BMB Rep.* **2011**, *44*, 410–414.

**Sample Availability:** Samples of the compounds in these studies are available from the authors.



© 2020 by the authors. Licensee MDPI, Basel, Switzerland. This article is an open access article distributed under the terms and conditions of the Creative Commons Attribution (CC BY) license (<http://creativecommons.org/licenses/by/4.0/>).